

Sorting of Mannose 6-Phosphate Receptors and Lysosomal Membrane Proteins in Endocytic Vesicles

Hans J. Geuze, Willem Stoorvogel, Ger J. Strous, Jan W. Slot, Jos E. Bleekemolen, and Ira Mellman*

Laboratory of Cell Biology, Medical School, University of Utrecht, The Netherlands; and

*Department of Cell Biology, Yale University School of Medicine, New Haven, Connecticut 06510

Abstract. The intracellular distributions of the cation-independent mannose 6-phosphate receptor (MPR) and a 120-kD lysosomal membrane glycoprotein (lgp120) were studied in rat hepatoma cells. Using quantitative immunogold cytochemistry we found 10% of the cell's MPR located at the cell surface. In contrast, lgp120 was not detectable at the plasma membrane. Intracellularly, MPR mainly occurred in the *trans*-Golgi reticulum (TGR) and endosomes. lgp120, on the other hand, was confined to endosomes and lysosomes. MPR was present in both endosomal tubules and vacuoles, whereas lgp120 was confined to the endosomal vacuoles. In cells incubated for 5–60 min with the endocytic tracer cationized ferritin, four categories of endocytic vacuoles could be discerned, i.e., vacuoles designated MPR⁺/lgp120⁻, MPR⁺/lgp120⁺, MPR⁻/lgp120⁺, and vacuoles nonimmunolabeled for MPR and lgp120. Tracer first reached MPR⁺/lgp120⁻, then MPR⁺/lgp120⁺, and finally MPR⁻/lgp120⁺ vacuoles, which are assumed to represent lysosomes.

To study the kinetics of appearance of endocytic tracers in MPR-and/or lgp120-containing pools in greater detail, cells were allowed to endocytose horseradish peroxidase (HRP) for 5–90 min. The reduction in detectability of MPR and lgp120 antigenicity on Western blots, due to treatment of cell homogenates with 3'3-diaminobenzidine, was followed in time. We found that HRP reached the entire accessible pool of MPR almost immediately after internalization of the tracer, while prolonged periods of time were required for HRP to maximally access lgp120. The combined data suggest that MPR⁺/lgp120⁺ vacuoles are endocytic vacuoles, intermediate between MPR⁺/lgp120⁻ endosomes and MPR⁻/lgp120⁺ lysosomes, and represent the site where MPR is sorted from lgp120 destined for lysosomes. We propose that MPR is sorted from lgp120 by selective lateral distribution of the receptor into the tubules of this compartment, resulting in the retention of lgp120 in the vacuoles and the net transport of lgp120 to lysosomes.

THE biogenesis of lysosomes involves the selective transport of newly synthesized lysosomal enzymes and membrane glycoproteins from the Golgi complex as well as the transport of extracellular macromolecules and perhaps certain membrane components internalized by endocytosis. Although the precise intracellular pathways and mechanisms underlying these transport events have yet to be established, considerable information has been obtained concerning the targeting of hydrolytic enzymes to lysosomes (Kornfeld, 1986; Sly and Fischer, 1982). After synthesis and core-glycosylation in the ER, most lysosomal enzymes acquire phosphorylated mannose residues in the Golgi complex which serve as the recognition marker for one of two mannose 6-phosphate receptors (MPR)¹ (Kornfeld, 1986; Stein et al., 1987). The receptor–ligand complexes are thought to exit the Golgi complex via coated buds at the *trans*-

Golgi reticulum (TGR) (Geuze et al., 1985) and arrive at an acidic post-Golgi compartment wherein the enzymes dissociate from the receptor and continue on to lysosomes, while the receptors return to the Golgi and/or the plasma membrane (Kornfeld, 1986; Von Figura and Hasilik, 1986). Recent evidence has suggested that this post-Golgi compartment may be endocytic in nature, and may be identical to endosomes (Helenius et al., 1983) or compartment of uncoupling receptor and ligand (CURL) (Geuze et al., 1984a, b; 1985; Brown et al., 1986; Pfeffer, 1987). However, the origin and function of this compartment have yet to be established. Since cell surface MPR can also mediate the transport of exogenous lysosomal enzymes to lysosomes via endocytosis, it would appear likely that the biosynthetic and endocytic pathways to lysosomes are connected in these endosome of CURL-like structures.

Although critical for the transport of newly synthesized and endocytosed lysosomal enzymes, the MPR itself is not found in the lysosomal membrane (Sahagian and Neufeld, 1983; Geuze et al., 1985; Brown et al., 1986; Von Figura et al., 1984) and thus must be efficiently sorted before reach-

1. *Abbreviations used in this paper:* BSAG, BSA complexed to 5 nm gold; CF, cationized ferritin; CURL, compartment of uncoupling receptor and ligand; DAB, diaminobenzidine; HRP, horseradish peroxidase; lgp(s), lysosomal glycoprotein(s); MPR, mannose 6-phosphate receptor; TGR, *trans*-Golgi reticulum.

ing lysosomes. Precisely the opposite occurs for a recently described class of lysosomal glycoproteins (lgps) which form the major constituents of the lysosomal membrane. These heavily sialylated and acidic integral membrane proteins are highly enriched in lysosomes, and are found in relatively small amounts in the Golgi complex, endosomes, or the plasma membrane (Lippincott-Schwartz and Fambrough, 1986, 1987; Reggio et al., 1984; Tougard et al., 1985; Lewis et al., 1985; Chen et al., 1985; Green et al., 1987; Barriocanal et al., 1986). One well-studied example is a 120-kD protein, designated lgp120, which appears to be sorted from newly synthesized plasma membrane proteins shortly after leaving the Golgi complex, reaches lysosomes with such speed that by-passage of the plasma membrane has been suggested (Green et al., 1987). However, the precise pathway of lgp120 transport, especially how it relates to the pathway of MPR-mediated lysosomal enzyme transport, has yet to be determined.

It seems likely that both lysosomal enzymes and lgps should share a common intracellular route to lysosomes. As mentioned above, it also seems likely that this route should cross-over with the endocytic pathway and that this interface should occur in a prelysosomal, post-Golgi organelle which would allow the selective recycling of MPR back to the Golgi or to the cell surface. Consequently, identifying the site at which the MPR is sorted from lgps may define a critical station in the biosynthetic and/or endocytic pathway to lysosomes.

Griffiths et al. (1988) have recently proposed that delivery of MPR and newly synthesized enzymes from TGR to lysosomes is mediated by a compartment which is endocytic in nature. In this study, we use quantitative immunocytochemical and biochemical approaches to define the morphology and the kinetics by which this compartment is accessed by endocytic tracers. Our results show that sorting of MPR and lgp120 occurs in endosomes.

Materials and Methods

Cells

H₄S cells, a continuous rat hepatoma cell line, were cultured in MEM containing 10% calf serum. H₄S cells were chosen for their relatively high content of both MPR and lgp120. For morphological studies, calf serum was replaced by 10% rabbit serum 16 h before use (Strous et al., 1985).

Experiments with Electron Dense Markers

Cells were incubated at 37°C for 10, 30, and 60 min in medium containing either 25 mg/ml dialyzed cationized ferritin (CF) (Miles Laboratories, Inc., Naperville, IL) or BSA complexed to 5 nm colloidal gold (BSAG). The final concentration of BSAG was ~50 gold particles per μm^3 culture medium. After incubation, the cells were briefly washed in fresh medium at 0°C and subsequently fixed in a mixture of 1% acrolein and 0.2% glutaraldehyde in 0.1 M phosphate buffer at pH 7.4. Cells were embedded in gelatin and stored in 2.3 M sucrose as described (Geuze et al., 1985).

Immunoelectronmicroscopy

Ultrathin cryosections of cells incubated with CF were indirectly immunosingle or -double labeled (Geuze et al., 1981; Slot and Geuze, 1984) with 6 and 9 nm protein A-gold particles (PAG6 and PAG9) prepared as previously described (Slot and Geuze, 1985). When the cells had been treated with 5 nm BSAG the sections were labeled with PAG¹⁰ and PAG¹⁵ for MPR and lgp120, respectively (Fig. 8). Routinely cathepsin D or albumin were double labeled with MPR or lgp120 as well. In double-labeling experiments the sequence of antibodies and gold probes was varied. Single labeling of

Table I. Distribution of MPR and lgp120 in H₄S Cells

Compartment	MPR	lgp120
Golgi stack	3	3
TGR	34	1
Dense buds, vesicles	18	—
Endosomes*	52	50
Tubules	16	—
Vacuoles	37	50
Irregular structures	—	10
Lysosomes†	—	36
Plasma membrane	10	1

Percentages of immunogold particles counted in cryosections of 20 cells, 10 each of two separate fixation experiments. Totals of 1,364 and 4,385 gold particles were counted for MPR and lgp120, respectively.

* Defined by the presence of MPR and endocytic tracer.

† Vacuoles with tracer and lgp120 but without MPR.

MPR, lgp120, and cathepsin D was performed using swine anti-rabbit IgG as an intermediate second antibody before PAG (Figs. 1-3, 7, and 9) because of its higher yield of gold particles (Geuze et al., 1987b). Characterizations of the polyvalent rabbit antibodies for the 215 kD cation-independent MPR and for cathepsin D (von Figura et al., 1984), albumin (Strous et al., 1983), and lgp120 (Lewis et al., 1985) have been described elsewhere. Finally, the sections were stained in uranyl acetate and embedded in methylcellulose.

Immunogold Quantitation of MPR and lgp120

Cells cultured in the absence of endocytic markers were used to estimate the subcellular distribution of MPR and lgp120. Sections double labeled for MPR and endogenous rat albumin and for lgp120 and albumin were selected for good morphology. In cell profiles all gold particles for MPR or lgp120 were counted and attributed to the ultrastructural features listed in Table I. Numbers of experiments, cells and gold particles are given in Table I. The presence of endogenous albumin served to distinguish TGR from endocytic structures (Geuze et al., 1985; Zijderhand-Bleekemolen et al., 1987). Each series of sections double labeled as above also included sections labeled for MPR and lgp120 for direct comparison of distributions. In these sections, label distributions were occasionally quantified as well, revealing MPR and lgp120 distributions very similar to those obtained from sections double labeled with either MPR or lgp120 and albumin (Table I). Background labeling as estimated from sections labeled with anti-amylase or without antibody, was <5% of specific labeling.

Quantitation of CF-containing Vacuoles

Cells treated for 5, 10, 30, and 60 min with CF at 37°C were used to score marker-containing vacuoles (endosomes, lysosomes) labeled for MPR only (MPR⁺/lgp120⁻), MPR and lgp120 (MPR⁺/lgp120⁺), lgp120 only (MPR⁻/lgp120⁺), or nonimmunolabeled. Only sections double labeled for MPR and lgp120 were used for this purpose. The selection of cells was as above. Numbers of experiments, and cells are given in Table II.

DAB-mediated Antigen Inactivation

Culture media of near confluent H₄S monolayers on 6-cm dishes were refreshed 1 d before the experiment. The cells were washed once with MEM containing 20 mM Hepes/NaOH, pH 7.2 (MEMH) at 37°C and were subsequently incubated at 37°C in MEMH containing horseradish peroxidase (HRP type VI; Sigma Chemical Co., St. Louis, MO). Nonendocytosed HRP was removed at 0°C by the following washing steps: four times quickly and once 30 min with MEMH, once quickly and once 60 min with 150 mM NaCl, 2 mM CaCl₂, 10 mM glycine, pH 9.0, twice quickly with MEMH, and once with homogenization buffer (0.25 M sucrose, 1 mM EDTA, 10 mM Hepes/NaOH, pH 7.2). We found that washing the cells at pH 9.0 caused dissociation of a significant amount of nonspecifically plasma membrane-bound HRP, probably due to the basic character of the HRP isoenzymes used. Cells were scraped in 0.5 ml homogenization buffer, and disrupted using a Dounce homogenizer (Kontes Glass Co., Vineland, NJ) with a tight fitting pestle. 3,3'-diaminobenzidine (DAB) treatment of the total homogenate was performed as described before (Stoorvogel et al., 1987),

Table II. Percentage of CF-positive Vacuoles Immunolabeled for MPR and Igpl20

Vacuoles	5 min CF	10 min CF	30 min CF	60 min CF
MPR ⁺ /Igpl20 ⁻	4	35	10	5
MPR ⁺ /Igpl20 ⁺	21	39	40	30
MPR ⁻ /Igpl20 ⁺	5	13	36	65
MPR ⁻ /Igpl20 ⁻	70	13	14	—

CF-containing endocytic vacuoles were classified into the four immunolabeling categories in the left column. Figures are percentages for each of the incubation experiments with CF. In two experiments, CF-containing vacuoles were counted in 83, 47, 50, and 41 cells incubated with CF at 37°C for 5, 10, 30, and 60 min, respectively.

except that the DAB concentration was 30 µg/ml instead of 1 mg/ml; at this concentration optimal protein cross-linking was obtained. A control sample from the same homogenate was incubated with DAB but without H₂O₂. Reactions were stopped by adding an equal volume of Laemmli sample buffer lacking reducing agents. The degree of loss of MPR and Igpl20 extractibility from the microsomes was measured using Western blotting. For the detection of MPR and Igpl20, respectively, 4 and 7.5% SDS-polyacrylamide gels (Laemmli, 1970) were used. Transfer to nitrocellulose sheets was obtained in 16 h at 30 V in a blotting apparatus (transblot cell; Bio-Rad Laboratories, Richmond, CA) using 25 mM sodium phosphate (pH 6.5) as transfer buffer. The nitrocellulose sheets were incubated in a 5% milk protein solution (a gift from Elk, DMV Campina BV, Bergeyk, Holland), and reacted with antiserum (1:200 diluted). Next the sheets were incubated in buffer containing ¹²⁵I-protein A. Protein A (P6650; Sigma Chemical Co.) was iodinated to 2–4 × 10⁶ cpm/µg (Stoorvogel et al., 1987). Quantitative detection of ¹²⁵I-protein A was performed by scanning the full lane width of a fluorographed film using an Ultrascan XL Enhanced Laser densitometer (LKB Instruments, Inc., Bromma, Sweden), or by counting the excised band in a gammacounter. The degree of Igpl20 and MPR loss was calculated by subtracting the quotient of the signals obtained from the incubations in the presence or the absence of H₂O₂ from 1.

Results

Subcellular Distribution of MPR and Igpl20

To establish the localization of the 215-kD MPR and Igpl20 in H₄S rat hepatoma cells we first quantitated the intracellular distribution of these two proteins by means of quantitative immunocytochemistry. These results are summarized in Table I. As previously found in the human hepatoma cell line HepG2 (Geuze et al., 1985), an important fraction (34%) of MPR resided in a reticulum of tubules associated with coated and uncoated electron dense buds and vesicles at the *trans*-face of the Golgi complex (Fig. 1). This compartment, termed *trans*-Golgi reticulum (TGR), was distinguished from endosomal tubules by the presence of endogenous newly synthesized albumin (Geuze et al., 1985; Zijderhand-Bleekemolen, 1987) and by the absence of the endocytic tracers CF and BSAG (see next section).

18% of the total cell MPR was concentrated in the electron dense buds and vesicles of TGR (Fig. 1). The buds often showed coated limiting membranes and contained cathepsin D as previously shown in HepG2 cells (Geuze et al., 1985). Due to the high concentration of MPR in the dense buds as compared to the intervening tubules, the MPR distribution in TGR was highly heterogenous (Fig. 1). Free dense vesicles similar in appearance to the dense TGR buds but uncoated, often surrounded endocytic vacuoles (Fig. 4). These vesicles also contained MPR (Fig. 4) and cathepsin D (Fig. 7) and may be involved in lysosomal enzyme transport. Igpl20, on

the other hand, could not be detected in the dense TGR buds and free vesicles. Stacked Golgi cisternae showed only 3% of both MPR and Igpl20 labeling. While 10% of the total cell MPR was localized at the plasma membrane, about half of which was in coated pits, virtually no Igpl20 labeling was observed in association with the cell surface.

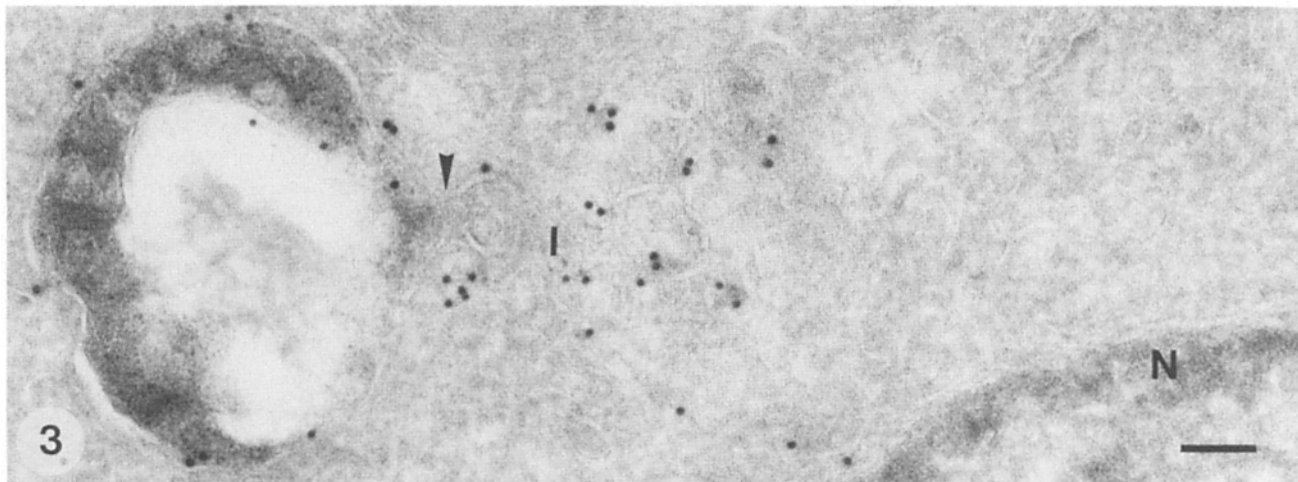
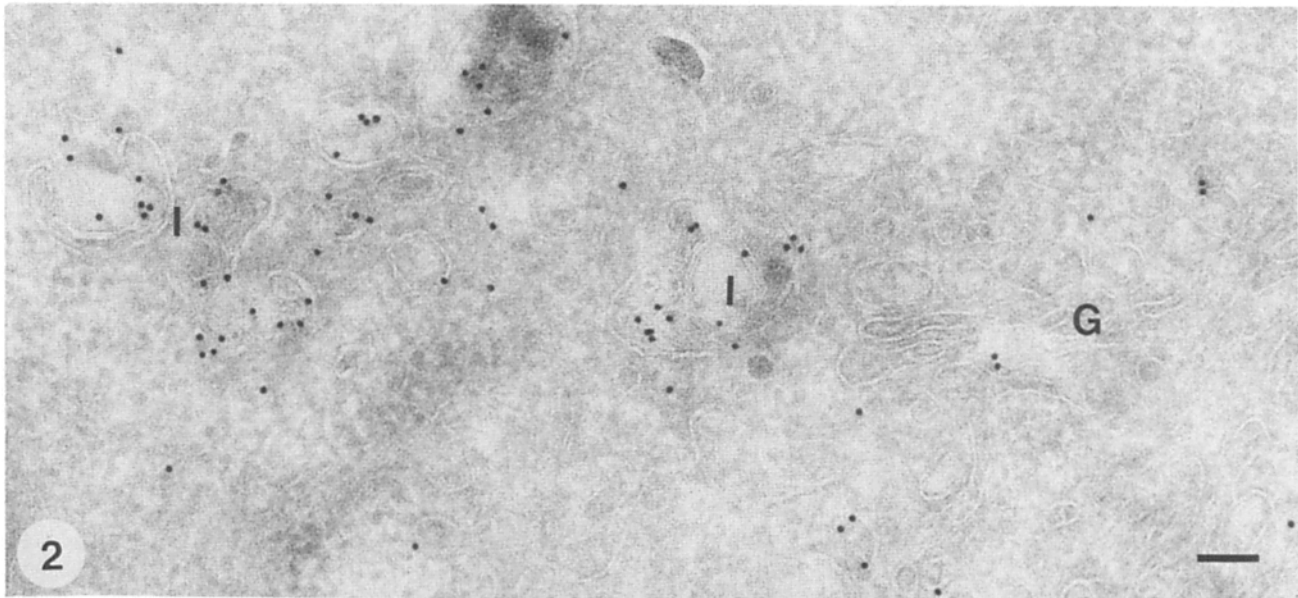
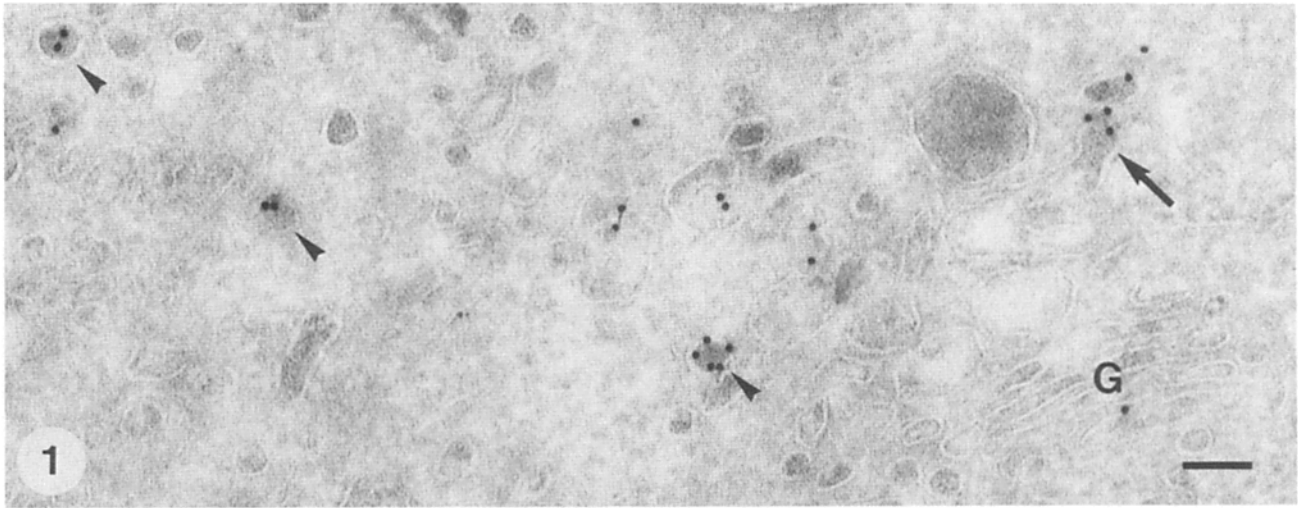
Major fractions of both MPR and Igpl20 were localized in endocytic structures and lysosomes. Since previous biochemical experiments have shown that dense, hydrolase-rich lysosomes are enriched in Igps (Lewis et al., 1985) and devoid of MPR (Von Figura et al., 1984; Sahagian and Neufeld, 1983), lysosomes were assumed to correspond to the Igpl20-positive and MPR-negative structures which accounted for up to 36% of the total cell Igpl20 labeling (Table I). These structures also contained the lysosomal enzyme cathepsin D. Igpl20⁺/MPR⁻ organelles were also characterized by the internal vesicles and electron dense material typical of lysosomes, and were readily labeled with endocytic tracers after long (30 min) incubations at 37°C (see below). A cathepsin D-labeled vacuole containing CF is shown in Fig. 7.

In addition to lysosomes, H₄S cells also contained tubules and vacuoles that were MPR-positive and Igpl20-negative, as well as structures that contained both markers (Figs. 4 and 5). These organelles were judged to be endocytic in origin since they could be labeled with endocytic tracers such as CF (Figs. 4 and 5) and were reminiscent of the prelysosomal organelle CURL previously defined in rat liver (Geuze et al., 1983, 1984b) and human HepG2 cells as an endocytic compartment in which the asialoglycoprotein receptor and its ligands uncouple (Geuze et al., 1985). Because asialoglycoprotein receptor is absent from H₄S cells, CURL function was not identified in these cells. Endosomal elements similar in morphology to CURL contained a substantial fraction (~50%) of both MPR and Igpl20. Interestingly, however, Igpl20 was not observed in CF-positive endosomal tubules, but only in the vacuolar portions (Fig. 6). MPR, on the other hand, was found in both the vacuolar and the tubular endosomal subcompartments (Figs. 6 and 9).

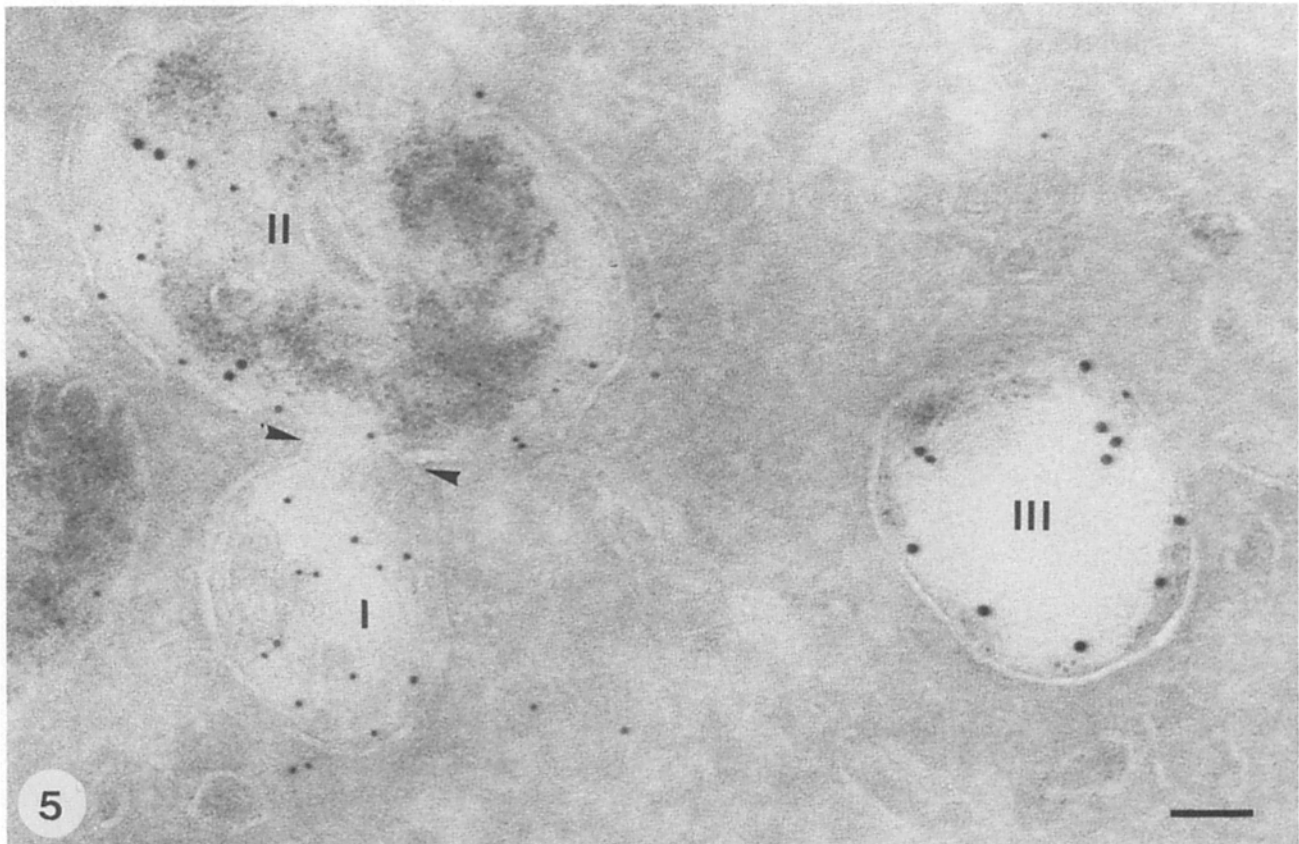
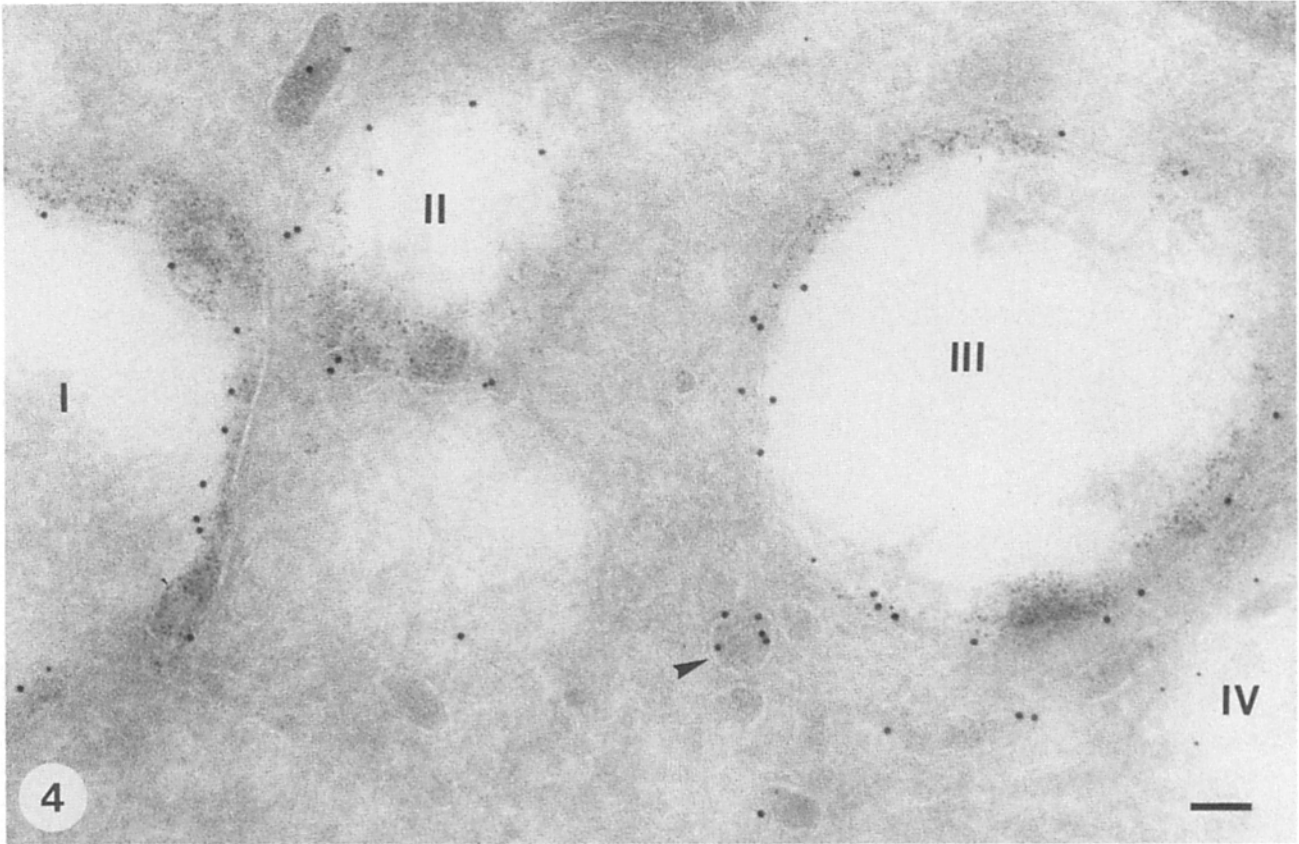
Finally, ~10% of the Igpl20 was present in structures of unknown origin. They consisted of tubules and vesicles and were found in the vicinity of lysosomes and endosomes in the Golgi region. They could not be labeled with CF (Figs. 2 and 3) and were thus judged not to be endocytic. These structures were also morphologically distinct from CF-positive endosomal tubules and vesicles, often contained internal membranes, and were MPR negative. Fig. 3 illustrates one such structure in apparent continuity with a lysosome. These irregular structures might represent a subpopulation of tubular lysosomes.

Appearance of Endocytic Tracers in MPR- and Igpl20-containing Endosomes

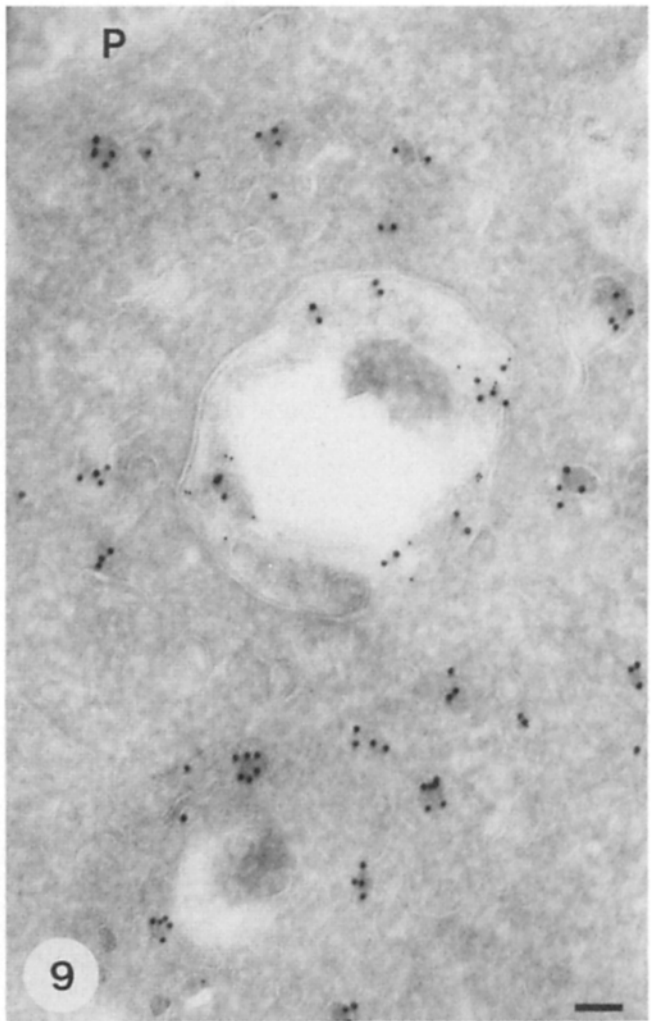
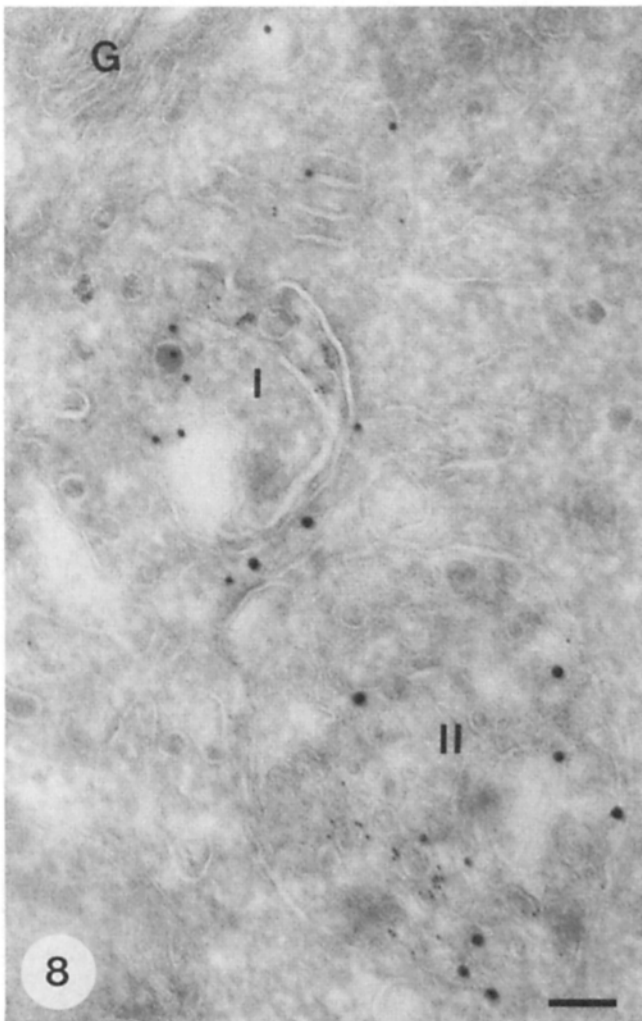
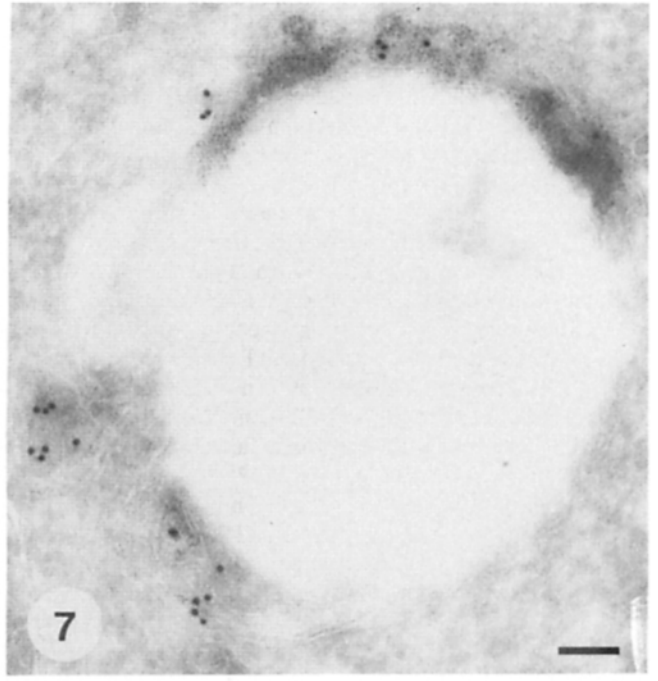
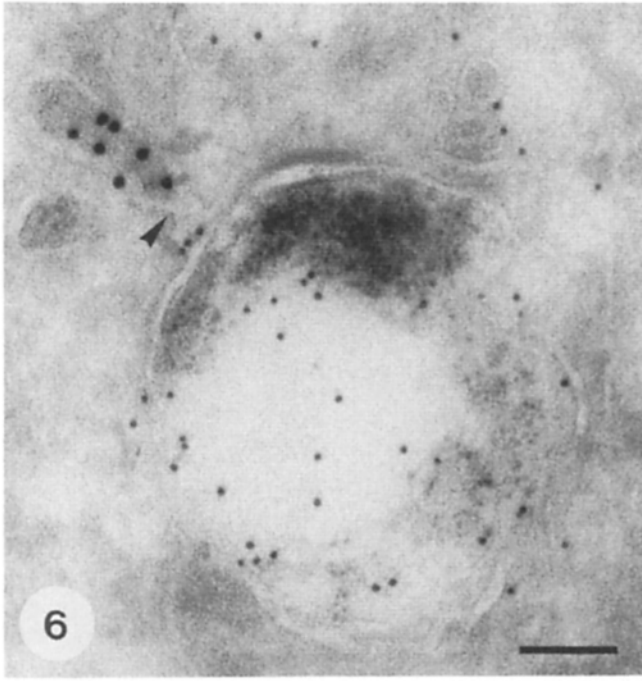
We next investigated whether the above distributions of MPR and Igpl20 in the endocytic pathway could further be defined by determining the sequence of appearance of endocytic markers in endosomes (i.e., MPR⁺/Igpl20⁻ and MPR⁺/Igpl20⁺ vacuoles) and lysosomes (i.e., MPR⁻/Igpl20⁺). Cells were incubated in media containing CF or BSAG, presumed to be nonspecific markers for nonspecific adsorptive (Danon et al., 1972) or fluid-phase endocytosis, respective-



Figures 1-3. (Fig. 1) 30-min CF, immunosingle labeling of MPR with PAG⁹. Golgi stack of cisternae (G), with, at its upper-left face, TGR showing a dense bud (*arrow*) and dense vesicles (*arrowheads*) with MPR. No CF is present in this field. Bar, 0.1 μ m. (Fig. 2) 30-min CF, immunosingle labeling of Igpl20 with PAG⁹. Igpl20 is present in irregularly shaped vesicles and tubules (*I*) at the lateral side of the Golgi stack (G). Bar, 0.1 μ m. (Fig. 3) 30-min CF, immunosingle labeling of Igpl20 with PAG⁹. A large CF-containing vacuole is continuous with irregularly shaped tubules at the arrowhead. Igpl20 is present in both the tubules and the vacuole. *N*, nucleus. Bar, 0.1 μ m.



Figures 4 and 5. (Fig. 4) 10-min CF, immunodouble labeling of MPR with PAG⁹ and Igpl20 with PAG⁶. Parts of four endosomes are shown. I, II, and III contain CF and show MPR labeling. In III a few particles for Igpl20 can be detected. IV lacks CF, but shows Igpl20 labeling only. Note the CF-negative dense vesicle with MPR (*arrowhead*) and the tubule with some CF of the upper left. Bar, 0.1 μ m. (Fig. 5) 30-min CF, immunodouble labeling of MPR with PAG⁹ and Igpl20 with PAG⁶. Vacuole III contains CF and MPR only, I lacks CF and shows Igpl20 only, whereas II contains all three markers. Vacuoles I and II seem in a process of fusion (*arrowheads*). Bar, 0.1 μ m.



ly, for 5, 10, 30, and 60 min at 37°C. After fixation, ultrathin frozen sections were prepared and double labeled using antibodies to MPR and Igpl20 as above. At each time point, CF-containing vesicles and tubules were scored as being positive for MPR, Igpl20, or both. Representative micrographs are shown in Figs. 4–9, and the quantitation of these data are given in Table II.

After 5 min of uptake CF was mainly present in MPR⁻/Igpl20⁻ vacuoles. Although at this time point 83 different cell profiles were examined, a too small number of immunolabeled vacuoles contained CF to get reliable data. However, CF had entered MPR-labeling vacuoles. Approximately 25% of the CF vacuoles showed MPR. After 10 min of uptake, CF was found in coated pits and in peripheral endosomes (Figs. 4 and 9). Of the CF-containing vacuoles 74% showed labeling for MPR, approximately half of which were MPR⁺/Igpl20⁻ and the other half MPR⁺/Igpl20⁺. After 30 and 60 min of uptake, CF occurred in large multivesicular endosomes and lysosomes (Figs. 3 and 5–8). By 30 min, the fraction of CF-contained structures that were positive for MPR had decreased to 50%; most of these were positive for both MPR and Igpl20 (40%); the remaining containing MPR only (10%). This trend continued such that after 60 min the fraction of vacuoles positive for both CF and MPR decreased to 35%, of which only 5% was scored as MPR⁺/Igpl20⁻ and the remainder (30%) as MPR⁺/Igpl20⁺. Thus, after longer periods of endocytosis, a progressively smaller percentage of CF-containing vacuoles contained MPR.

The opposite situation was found for Igpl20-positive structures (Table II). After 5 min of CF uptake 25% of the CF vacuoles showed Igpl20 and after 10 min about half of the CF-positive vacuoles contained Igpl20, only 13% of which did not also contain MPR. By 30 and 60 min of uptake, however, Igpl20 occurred in 76 and 95% of the CF-positive vacuoles, respectively. At the 60-min time point, 65% of the CF-positive vacuoles were judged as being cytochemically demonstrable lysosomes, i.e., MPR⁻/Igpl20⁺ vacuoles, with the bulk of the remainder being MPR⁺/Igpl20⁺ structures.

Taken together, these results show that endocytic tracers en route to lysosomes pass through endosomes that become progressively depleted in MPR and progressively enriched in Igpl20. They also suggest that the MPR⁺/Igpl20⁺ structures occupy an intermediate position between MPR⁺/Igpl20⁻ endosomes and MPR⁻/Igpl20⁺ lysosomes. It seems likely, therefore, that they may correspond to the intracellular site at which MPR and Igpl20 are sorted before the delivery of internalized material to lysosomes. It is notable that the relative size of this class of vacuoles is maximal after 10 min of CF uptake, suggesting that the sorting of MPR from the endocytic route takes place after 10 min of uptake.

Kinetics of HRP Appearance in MPR- and Igpl20-containing Endosomes

In the previous section, endocytic marker-positive vacuoles were scored for the presence of MPR and/or Igpl20. In this section a “mirror experiment” was performed in which MPR- and/or Igpl20-positive vacuoles were scored for the presence of an endocytic marker. To this purpose, we established a quantitative biochemical assay to determine the degree of colocalization of the two markers with a well-characterized fluid phase endocytic tracer, HRP. The assay took advantage of the observation that incubating HRP-containing vesicles with DAB and H₂O₂ results in the formation of insoluble polymers (Courtroy et al., 1984), which reduce the ability to detect a variety of protein antigens (Ajioka and Kaplan, 1987).

We first demonstrated that the HRP-DAB reaction product could be used to interfere with the detection of both MPR and Igpl20. H₂S cells were incubated for 30 min in medium containing HRP at concentrations up to 3 mg/ml before homogenization and addition of DAB and H₂O₂. The reactions were terminated by the addition of SDS. The proteins were separated by SDS-PAGE, and the antigenicity of MPR and Igpl20 was analyzed on Western blots. As shown in Fig. 10, the degree of inactivation of both antigens was dependent on HRP concentration, being maximal at 1.5 mg/ml. These results indicated that the maximal amount of MPR and Igpl20 accessible to HRP could be inactivated at HRP concentrations of 3 mg/ml.

We next determined the kinetics of entrance of HRP into MPR- and Igpl20-containing vesicles by incubating H₂S cells in HRP-containing medium for various periods of time at 37°C before homogenization and Western blot analysis. As shown in Fig. 11, as much as 10–15% of the MPR immunoreactivity had disappeared after only 5 min of HRP uptake. This represented the maximum amount of inactivation since MPR reactivity did not further decrease after longer periods of HRP uptake. In contrast, only a small decrease in Igpl20 immunoreactivity was observed after 5 min, with the amount of antigenic inactivation increasing continuously as a function of time of HRP uptake. Some Igpl, however, was also present in early endosomal structures, as there was no lag time in the inactivation curve. Half of the total cellular Igpl pool was accessed by HRP after 45–60 min uptake. By 90 min, the amount of immunoreactive Igpl20 has decreased maximally representing 30% of the initial signal. Thus, HRP reached the entire accessible pool of MPR-containing endosomes almost immediately after internalization, while prolonged periods of time were required for HRP to access Igpl20-containing vesicles.

Figures 6–9. (Fig. 6) 30-min CF, immunodouble labeling of MPR with PAG⁹ and of Igpl20 with PAG⁶. The CF-containing vacuole shows only Igpl20 whereas the tubule, which seems in continuity with the vacuole (*arrowhead*) lacks CF but contains MPR. Close to the tubule is a nonimmunolabeled vesicular profile with some CF. Bar, 0.1 μm. (Fig. 7) 30-min CF, immunosingle labeling of cathepsin D with PAG⁹. The somewhat swollen vacuole contains CF and cathepsin D labeling at its periphery. Note the dense vesicle with cathepsin D in close proximity to the vacuolar membrane. Bar, 0.1 μm. (Fig. 8) 30-min BSAG⁵, immunodouble labeling of MPR with PAG¹⁰ and Igpl20 with PAG¹⁵. Close to the Golgi complex (*G*) two multivesicular endosome profiles I and II can be discerned, I probably being cut tangentially. Both bodies show BSAG⁵, together with MPR and Igpl20 labeling. Note the dense vesicle close to I. Some BSAG⁵ particles can be seen with a tubule. Bar, 0.1 μm. (Fig. 9) 10-min BSAG⁵, immunosingle labeling of MPR with PAG⁹. A vacuole close to the plasma membrane (*P*) shows both BSAG⁵ and MPR labeling. Note the MPR-positive dense vesicles and tubules surrounding the vacuole. Bar, 0.1 μm.

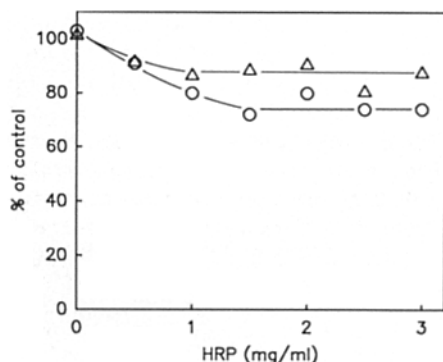
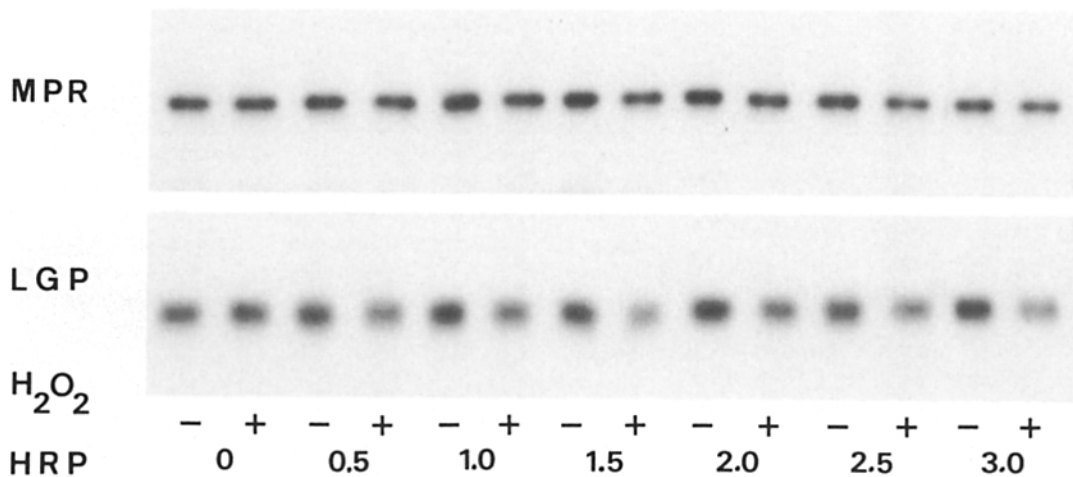


Figure 10. The effect of DAB cytochemistry on the extractability of Igpl20 and MPR as a function of HRP concentration. H₄S cultures were incubated for 30 min in medium with various concentrations of HRP. Samples of homogenates were incubated in DAB solution without (–) or with (+) H₂O₂. Noncaptured Igpl20 and MPR (+H₂O₂) were visualized with Western blotting (*top*), quantified, and expressed as percentages of the totals (–H₂O₂) (*bottom curves*). For both Igpl20 (○) and MPR (Δ) saturation of quenching is reached at 3 mg/ml HRP medium.

To demonstrate the specificity of this approach, a control experiment was also performed in which two plates of cells, only one of which was incubated in HRP-containing medium for 90 min, were scraped and combined before homogenization, and processing as above. As shown in Fig. 11 (*solid symbols*) an intermediate value of antigenic inactivation was obtained for both Igpl20 and MPR. Thus, the HRP-DAB reaction product did not result in the nonselective inactivation of antigen in vacuoles that did not contain HRP.

Taken together, the HRP inactivation data confirm the results of the immunocytochemical experiments concerning the relative distribution of MPR and Igpl20 on the endocytic pathway. Both the electron microscopic and biochemical approaches show that MPR as well as Igpl20 are found in endocytic organelles. They also indicate that both proteins are reached by endocytic tracers shortly after internalization, although a progressively greater fraction of Igpl20 is encountered as endocytic tracers move on to the lysosomes.

Discussion

The present results show that significant pools of both MPR and Igpl20 exist in prelysosomal organelles in H₄S cells. By immunocytochemistry we found approximately half of the MPR in endosomes in agreement with previous qualitative immunocytochemical observations in other cell types (Geuze et al., 1984a, 1985). Endosomal vacuoles contained 37% and endosomal tubules 16% of the MPR (Table I). On the other hand, the HRP-DAB inactivation experiments showed

that, after as little as 5 min of continuous HRP uptake, the maximal amount of endosomal MPR (~15% of the total cellular MPR; Fig. 11), is encountered. It was expected that a larger fraction of the MPR was accessible to HRP. A possible explanation for the discrepancy between the immunocytochemical and HRP quenching data for MPR might be that MPR, recycling between the Golgi complex and endosomes (the majority of this receptor) tends in the direction of the tubular system, thus escaping DAB cross-linking. As surface derived MPR (10–15% of total cell MPR) are recycling, it could well be that only these receptors are effectively quenched by endocytosed HRP. In contrast to MPR, continuously more Igpl20 was reached by HRP and cationized ferritin during prolonged uptake. In the same experiment Igpl20 is almost completely accessible for HRP (50% in endosomal vacuoles), as a fluid phase endocytic marker presumably localizes to the vacuoles. While much of this Igpl20 was encountered after delivery to lysosomes, the immunocytochemical data show that significant amounts of this lysosomal protein was found in prelysosomal, MPR-containing structures.

Upon increasing incubation time with CF, the relative amount of CF-positive MPR⁺/Igpl20⁻ vacuoles decreased compared with CF-positive MPR⁺/Igpl20⁺ vacuoles (Table II). This shows that the former type is labeled before the latter one. In these immunocytochemical experiments endocytic marker-positive vacuoles were quantitated for the presence of MPR and/or Igpl20 whereas in the biochemical experiments MPR or Igpl20 were quantitated for their presence in vacuoles also containing an endocytic marker. To-

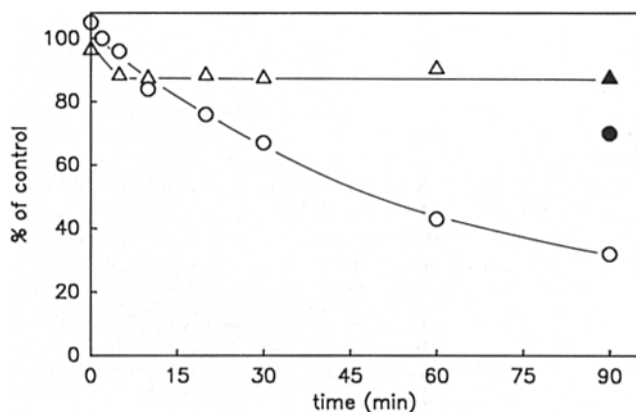
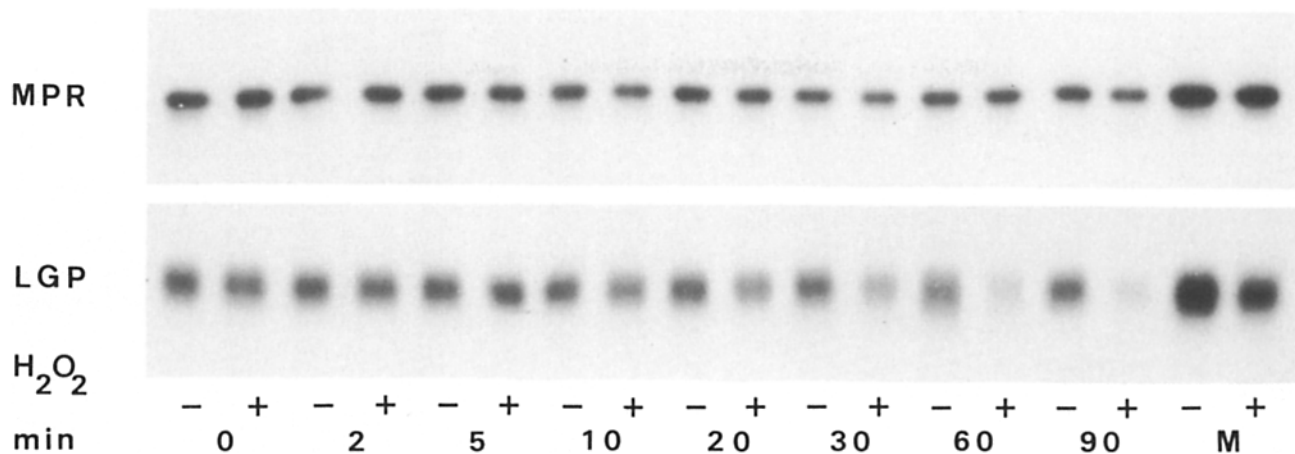


Figure 11. The accessibility of lgpl20 (○) and MPR (△) by endocytosed HRP as a function of time. Cultures were incubated for various periods of time in medium containing 3 mg/ml HRP. Samples of homogenates were incubated in DAB solution without (–) or with (+) H₂O₂. Noncaptured lgpl20 and MPR (+H₂O₂) were visualized using Western blotting (top), quantified and plotted as percentages of the totals (–H₂O₂) (bottom). The specificity of the procedure is shown by the mix experiment at 90 min (M) (●, ▲, see text).

gether the results of these mirror experiments show that the endocytic markers first quickly label a limited fraction of the MPR-containing compartments followed by a further increase in endocytic marker-positive vacuoles that also contain lgpl20 or contain lgpl20 only. It is clear that endocytic tracers appear in MPR⁺/lgpl20⁻ and MPR⁺/lgpl20⁺ structures before reaching MPR⁻/lgpl20⁺ lysosomes. Whether CF and HRP pass from MPR⁺/lgpl20⁻ through the MPR⁺/lgpl20⁺ structures, possibly corresponding to one or more populations of late endosomes (Schmid et al., 1988), before reaching MPR⁻/lgpl20⁺ lysosomes cannot be definitely determined. Free flow electrophoresis has shown that endocytic tracers begin to enter "late endosomes" after only a brief (1–2 min) lag (Schmid et al., 1988), consistent with the appearance of CF in MPR⁺/lgpl20⁺ vacuoles within 10 min. Transport of endocytic tracers through late endosomes is also highly asynchronous (Schmid et al., 1988) consistent with the small decrease in the fraction of CF in the MPR⁺/lgpl20⁺ structures. The most likely explanation for the differences in labeling kinetics and lgpl20 vs. MPR distribution is that MPR escapes transport to lysosomes by being sorted from this late endosomal compartment. According to the definition used here, lgpl20 is not exclusively a lysosomal protein. Since 50% of the total cell lgpl20 was colocalized in vacuoles containing MPR, and since MPR has been shown not to occur in dense, hydrolase-rich lysosomes (Sahagian and Neufeld, 1983; Von Figura et al., 1984) it is apparent that as much as half of all lgpl20 in H₂S cells is present in the nonlysosomal MPR⁺/lgpl20⁺ structures. While this class of MPR⁺/lgpl20⁺ vacuoles was not de-

tected by double immunofluorescence using antibodies to MPR and lgpl20 (Brown et al., 1986), they are in many respects similar to the MPR⁺/lgpl20⁺ structures recently identified by immunocytochemistry in normal rabbit kidney cells (Griffiths et al., 1988). The large nonlysosomal lgpl20 pool cannot account for newly synthesized protein on transport to lysosomes. The half-life of lgpl20 is 10–20 h depending on cell type, and transport of newly synthesized lgpl20 to organelles cofractionating with lysosomes in Percoll gradients is very fast (Green et al., 1987). The nature of this lgp is unknown. One explanation is that lgpl20 is not only a resident of the lysosomes but also of a "late" endosomal compartment. Another possibility is that lgpl20 shuttles between the two compartments, a similar situation as described for lep100, a lysosomal membrane protein of avian fibroblasts (Lippincott-Schwartz and Fambrough, 1987).

MPR⁺/lgpl20⁺ vacuoles constitute the prelysosomal endosomal compartment from which MPR is not yet completely sorted. Previous EM immunocytochemical results have demonstrated that in normal rabbit kidney cells, endocytic tracers fail to reach lgpl20-positive vacuoles when the cells are incubated at 20°C (Griffiths et al., 1985) a condition known to block the transfer of internalized material from endosomes to lysosomes (Dunn et al., 1980). These conditions were also shown to block the transfer of newly synthesized lgps to lysosomes (Green et al., 1987). Because low temperature may block other lgp pathways in addition to the endocytic route, it is conceivable that under these experimental conditions the lgp distribution is different from normal. On the basis of low temperature experiments Griffiths et al.

(1988) termed the MPR⁺/lgpl20⁺ compartment postendosomal and prelysosomal. Given that the MPR⁺/lgpl20⁺ vacuoles appear to constitute a class of vacuoles intermediate in composition, and in kinetics, between MPR⁺/lgpl20⁻ endosomes and MPR⁻/lgpl20⁺ lysosomes, our data and those of Griffiths et al. (1988) suggest that this compartment represents the ultimate prelysosomal endosomal compartment. Our present quantitative biochemical and immunocytochemical data document that the MPR⁺/lgpl20⁺ structures represent a major station on the endocytic pathway; the kinetic data also support the possibility that the MPR⁺/lgpl20⁺ endosomes serve as an obligatory intermediate on the pathway to lysosomes.

In addition to differences in organelle localization, MPR and lgpl20 were also differentially distributed within individual organelles. MPR was found in both tubules and vacuoles, whereas lgpl20 was limited only to the vacuolar portions of endosomes. The existence of tubular and vacuolar domains of endosomes has been well established (Marsh et al., 1986; Gonnella and Neutra, 1984; Christensen, 1982; Geuze et al., 1983, 1987a; van Deurs, 1984) although the function of these specializations remains incompletely understood. What little information exists suggests that the tubular elements of endosomes form the nascent recycling vesicles which mediate the transport of internalized receptors and certain ligands back to the plasma membrane. Endosomal vacuoles, on the other hand, are thought to mediate transport of internalized material to lysosomes. For example, when renal proximal tubule cells or cultured fibroblasts internalize CF, endosomal vacuoles are the first elements labeled. With increasing time, however, CF-containing tubules become more abundant, suggesting that the tubules derive from the vacuoles (Christensen, 1982; van Deurs, 1984).

These findings are in agreement with our observations on the asialoglycoprotein receptor and MPR in hepatocytes and HepG2 hepatoma cells (Geuze et al., 1983, 1984a, 1985). Both receptors recycle many times during their lifetimes, and by immunocytochemistry can be demonstrated to exist in higher densities in endosomal tubules than in endosomal vacuoles. While such careful quantitation has not yet been performed in the H₄S rat hepatoma cells used here, endosomes often showed the highest density of MPR labeling in endosomal tubular elements. On the other hand, lgpl20 labeling was found in highest density in the vacuolar elements, being scarcely present in the tubules. In light of the possible role for endosomal tubules in membrane recycling, these findings suggest that MPR may be sorted from lgpl20 by selective lateral distribution of the receptor into the tubules, effectively resulting in the retention of lgpl20 in the vacuoles and, accordingly, in the net transport of lgps to lysosomes.

Our results do not present direct evidence as to which type of organelle is engaged in the delivery of newly synthesized lysosomal enzymes to lysosomes. However, the presence of both MPR and cathepsin D in dense vesicles similar in appearance and immunolabeling to buds at the TGR and which surround endosomes suggests that these dense vesicles represent the post-Golgi transport vehicles of MPR-ligand complexes.

In summary, we have identified a unique, previously unexpected class of endocytic vacuoles intermediate in composi-

tion and kinetics between MPR⁺/lgpl20⁻ endosomes and MPR⁻/lgpl20⁺ lysosomes. They presumably represent an endosomal site at which internalized MPR is sorted from lgps and content proteins destined for lysosomes.

The authors thank Janice Griffith for excellent technical assistance, Tom van Rijn for preparing the photographs, and Eli de Bruijn for taking care of the manuscript.

The work was supported by grant 900-523-094 of Medigon, The Hague, Holland.

Received for publication 25 March 1988, and in revised form 19 July 1988.

References

- Ajioka, R. S., and J. Kaplan. 1987. Characterization of endocytic compartments using the horseradish peroxidase-diaminobenzidine density shift technique. *J. Cell Biol.* 104:77-85.
- Barriocanal, J. G., J. S. Bonifacino, L. Yuan, and I. V. Sandoval. 1986. Biosynthesis, glycosylation, movement through the Golgi system and transport to lysosomes by a N-linked carbohydrate independent mechanism of three lysosomal integral membrane proteins (LIMPs). *J. Biol. Chem.* 261:1604-1607.
- Brown, W. J., J. Goodhouse, and M. G. Farquhar. 1986. Mannose-6-phosphate receptors for lysosomal enzymes cycle between the Golgi complex and endosomes. *J. Cell Biol.* 103:1235-1247.
- Chen, J. W., T. L. Murphy, M. C. Willingham, I. Pastan, and J. T. August. 1985. Identification of two lysosomal membrane glycoproteins. *J. Cell Biol.* 101:85-95.
- Christensen, E. I. 1982. Rapid membrane recycling in renal proximal tubule cells. *Eur. J. Cell Biol.* 29:43-49.
- Courtney, P. J., J. Quintart, and P. Baudhuin. 1984. Shift of equilibrium density induced by 3,3'-diaminobenzidine cytochemistry: a new procedure for the analysis and purification of peroxidase-containing organelles. *J. Cell Biol.* 98:870-876.
- Danon, D., L. Goldstein, Y. Marikovsky, and E. Skutelsky. 1972. Use of cationized ferritin as a label of negative charges on cell surfaces. *J. Ultrastruct. Res.* 38:500-510.
- Dunn, W. A., A. L. Hubbard, and N. N. Aronson. 1980. Low temperature selectively inhibits fusion between pinocytotic vesicles and lysosomes during heterography of ¹²⁵I asialofetuin by the perfused rat liver. *J. Biol. Chem.* 255:5971-5978.
- Geuze, H. J., J. W. Slot, and A. L. Schwartz. 1987a. Membranes of sorting organelles display lateral heterogeneity in receptor distribution. *J. Cell Biol.* 104:1715-1723.
- Geuze, H. J., J. W. Slot, G. J. A. M. Strous, A. Hasilik, and K. Von Figura. 1984a. Ultrastructural localization of the mannose 6-phosphate receptor in rat liver. *J. Cell Biol.* 98:2047-2055.
- Geuze, H. J., J. W. Slot, G. J. Strous, A. Hasilik, and K. Von Figura. 1985. Possible pathways for lysosomal enzyme delivery. *J. Cell Biol.* 101:2253-2262.
- Geuze, H. J., J. W. Slot, G. J. Strous, H. F. Lodish, and A. L. Schwartz. 1983. Intracellular site of asialoglycoprotein receptor-ligand uncoupling: double-label immunoelectron microscopy during receptor-mediated endocytosis. *Cell.* 32:277-287.
- Geuze, H. J., J. W. Slot, G. J. Strous, J. Peppard, K. Von Figura, A. Hasilik, and A. L. Schwartz. 1984b. Intracellular receptor sorting during endocytosis: comparative immunoelectron microscopy of multiple receptors in rat liver. *Cell.* 37:195-204.
- Geuze, J. J., J. W. Slot, P. A. Van der Ley, and R. C. T. Scheffer. 1981. Use of colloidal gold particles in double-labeling immunoelectron microscopy on ultrathin frozen sections. *J. Cell Biol.* 89:653-665.
- Geuze, H. J., J. W. Slot, K. Yanagibashi, J. A. McCracken, A. L. Schwartz, and P. F. Hall. 1987b. Immunogold cytochemistry of cytochromes P-450 in porcine adrenal cortex: two enzymes (side-chain cleavage and 11 beta-hydroxylase) are co-localized in the same mitochondria. *Histochemistry.* 86:551-557.
- Gonnella, P. A., and M. R. Neutra. 1984. Membrane-bound and fluid-phase macromolecules enter separate prelysosomal compartments in absorptive cells of suckling rat ileum. *J. Cell Biol.* 99:909-917.
- Green, S. A., K.-P. Zimmer, G. Griffiths, and I. Mellman. 1987. Kinetics of intracellular transport and sorting of lysosomal membrane and plasma membrane proteins. *J. Cell Biol.* 105:1227-1240.
- Griffiths, G., S. Pfeiffer, K. Simons, and K. Matlin. 1985. Exit of newly synthesized membrane proteins from the trans-cisterna of the Golgi complex to the plasma membrane. *J. Cell Biol.* 101:949-964.
- Griffiths, G., B. Hoflack, K. Simons, I. Mellman, and S. Kornfeld. 1988. The mannose 6-phosphate receptor and the biogenesis of lysosomes. *Cell.* 52:329-341.

- Helenius, A., I. Mellman, D. Wall, and A. Hubbard. 1983. Endosomes. *Trends Biochem. Sci.* 7:245-249.
- Kornfeld, S. 1986. Trafficking of lysosomal enzymes in normal and disease states. *J. Clin. Invest.* 77:1-6.
- Laemmli, U. K. 1970. Cleavage of structural proteins during the assembly of the head of bacteriophage T4. *Nature (Lond.)* 227:680-685.
- Lewis, V., S. A. Green, M. Marsh, P. Vihko, A. Helenius, and I. Mellman. 1985. Glycoproteins of the lysosomal membrane. *J. Cell Biol.* 100:1839-1847.
- Lippincott-Schwartz, J., and D. M. Fambrough. 1986. Lysosomal membrane dynamics: structure and intraorganellar movement of a major lysosomal membrane glycoprotein. *J. Cell Biol.* 102:1593-1605.
- Lippincott-Schwartz, J., and D. M. Fambrough. 1987. Cycling of the integral glycoprotein, LEP 100, between plasma membrane and lysosomes: kinetic and morphological analysis. *Cell* 49:669-677.
- Marsh, M., G. Griffiths, G. E. Dean, I. Mellman, and A. Helenius. 1986. Three-dimensional structure of endosomes in BHK-21 cells. *Proc. Natl. Acad. Sci. USA* 83:2899-2903.
- Pfeffer, S. R. 1987. The endosomal concentration of a mannose 6-phosphate receptor is unchanged in the absence of ligand synthesis. *J. Cell Biol.* 105:229-234.
- Reggio, H., D. Bamton, E. Harms, E. Condrier, and D. Louvard. 1984. Antibodies against lysosomal membranes reveal a 100,000-mol-wt protein that cross reacts with purified H⁺, K⁺ ATP-ase from gastric mucosa. *J. Cell Biol.* 99:1511-1526.
- Sahagian, G. G., and E. F. Neufeld. 1983. Biosynthesis and turnover of the mannose 6-phosphate receptors in cultured Chinese Hamster Ovary cells. *J. Biol. Chem.* 258:7121-7128.
- Schmid, S. L., R. Fuchs, P. Male, and I. Mellman. 1988. Two distinct subpopulations of endosomes involved in membrane recycling and transport to lysosomes. *Cell* 52:73-83.
- Slot, J. W., and H. J. Geuze. 1984. Gold markers for single label and double immunolabeling of ultrathin cryosections. In *Immunolabelling for Electron Microscopy*. J. M. Polak and J. M. Vardell, editors. Elsevier Sc Pub. B. V., Amsterdam. 129-142.
- Slot, J. W., and H. J. Geuze. 1985. A new method of preparing gold probes for multiple-labeling cytochemistry. *Eur. J. Cell Biol.* 38:87-93.
- Sly, W. S., and H. D. Fischer. 1982. The phosphomannosyl recognition system for intracellular and intercellular transport of lysosomal enzymes. *J. Cell Biochem.* 18:67-85.
- Stein, M., J. E. Zijderhand-Bleekemolen, H. J. Geuze, A. Hasilik, and K. von Figura. 1987. Mr 46000 mannose 6-phosphate specific receptor: its role in targeting of lysosomal enzymes. *EMBO (Eur. Mol. Biol. Organ.) J.* 6:2677-2681.
- Stoorvogel, W., H. J. Geuze, and G. J. Strous. 1987. Sorting of endocytosed transferrin and asialoglycoprotein occurs immediately after internalization in HepG2 cells. *J. Cell Biol.* 104:1261-1268.
- Strous, G. J., A. Du Maine, J. E. Zijderhand-Bleekemolen, J. W. Slot, and A. L. Schwartz. 1985. Effect of lysosomotropic amines on the secretory pathway and on the recycling of the asialoglycoprotein receptor in human hepatoma cells. *J. Cell Biol.* 101:531-539.
- Strous, G. J., P. van Kerkhof, R. Willemsen, H. J. Geuze, and E. G. Berger. 1983. Transport and topology of galactosyltransferase in endomembranes of HeLa cells. *J. Cell Biol.* 97:723-727.
- Tougaard, C., D. Louvard, R. Picart, and A. Tixier-Vidal. 1985. Antibodies against a lysosomal membrane antigen recognize a prelysosomal compartment involved in the endocytic pathway in cultured prolactin cells. *J. Cell Biol.* 100:786-793.
- van Deurs, B. 1984. Endocytosis in kidney proximal tubules cells and cultured fibroblasts: a review of the structure aspects of membrane recycling between the plasma membrane and endocytic vacuoles. *Eur. J. Cell Biol.* 33:163-173.
- Von Figura, K., and A. Hasilik. 1986. Lysosomal enzymes and their receptors. *Annu. Rev. Biochem.* 55:167-193.
- Von Figura, K., V. Gieselmann, and A. Hasilik. 1984. Antibody to mannose 6-phosphate specific receptor induces receptor deficiency in human fibroblasts. *EMBO (Eur. Mol. Biol. Organ.) J.* 3:1281-1286.
- Zijderhand-Bleekemolen, J., A. L. Schwartz, J. W. Slot, G. J. Strous, and H. J. Geuze. 1987. Ligand- and weak base-induced redistribution of asialoglycoprotein receptors in hepatoma cells. *J. Cell Biol.* 104:1647-1654.